Weather sensitive load flow analysis of radial distribution system

M. KUMARI[1], S. SWAPNIL[2], R. RANJAN[3] AND V. R. SINGH[4]

[1]UIET, MDU, Dept. of Electrical Engg., Rohtak, Haryana, INDIA

[2] University of Florida, Department of Computer & Information Science & Engineering, Gainesville, USA

[3]Professor & Director, IITB Sonipat, Haryana, INDIA

[4]PDMCE, MDU, Dept. of Electrical Engg, Bahadurgarh, Haryana, INDIA

[1]meena_dhillon26@yahoo.com, [2]shubham.swapnil94@gmail.com ,[3]r_ranjan66@yahoo.com,

[4]vrsingh@ieee.org

Abstract: -In conventional load flow analysis, the branch resistances of the test system are considered fixed, despite of the fact that they are temperature and weather conditions dependent. For accurate calculation of power losses and to improve the efficiency of load flow solutions, the effect of ambience conditions on branch resistance should be considered. In this paper, an attempt has been made to incorporate a weather condition while solving radial distribution systems and a modified load flow algorithm is presented that is weather sensitive. This has been tested on Several IEEE RDS system. The results are compared with conventional load flow method and a noticeable change in the active power loss and node voltages were observed when Resistance is considered as a fixed parameter than weather sensitive.

Key-Words: - Conventional load flow analysis(CLFA), radial distribution system, Weather sensitive load flow analysis(WSLFA).

1 Introduction

Load flow study is the important tool for planning, designing and operation of a power system. From past decades many researchers have developed conventional algorithms for solving power flow problems [1]-[4]. In conventional study the researchers have taken line parameters as a constant but in reality resistance is the function of branch temperature and current. The temperature of the overhead conductor is depends upon the weather condition (ambient temp, wind speed and direction, solar intensity, azimuth angle etc.) and load current magnitude [5]-[11]. Under the extreme weather condition the parameters of power system yield significant deviation, especially conductor temperature, resistance, node voltage and loss. Thus temperature is an important aspect in load flow calculation.

In conventional load flow study the rise in branch temperature is neglected. So, the results comes out from these studies are erroneous. To reduce errors in state estimation and power flow, temperature effect should be considered in power flow calculation.

From past few decades, researcher have proposed some methods incorporating temperature variation effect in power flow calculation such as electro thermal coordination(ETC)[6]-[7] and parameter estimation [8]. In [8] the authors proposed an algorithm with resistance correction module that utilizes weather data and the heat balance equation. By incorporating available weather condition information within the line model, more accurate results can be expected from the state estimation tools and the energy management system.

This paper focus on the influence of environmental factor on conductor resistance and, as a consequence, on the load flow studies of radial distribution systems. Section 2 describe the electro thermal model of the system and estimated the conductor temperature.

In section 3, a Modified load flow algorithm is presented which estimate the system states. The

algorithm first solve the conventional load flow considering resistance as constant and then computed the branch temperature based upon the load flow results and update the conductor temperature and resistance. To find the accurate value of line resistance, a methodology based on repeated load flow solutions is adopted. Section 4 shows the results of test cases that a noticeable change in the active power loss and node voltage occur when updated resistances corresponding to estimated conductor temperatures are employed rather than constant resistances.

2. Electro thermal model of power system

The resistance of the conductor is the function of temperature according to [9]

$$\boldsymbol{R = R_{ref}\frac{T_C+T_F}{T_{ref}+T_F}} \quad (1)$$

Where

R is the conductor resistance at temperature $\boldsymbol{T_C}$,
$\boldsymbol{T}_C$ is the conductor temperature,
R_{ref} is the conductor resistance at the reference temperature
T_{ref} is the reference temperature
T_F is temperature constant of the metal (228.1℃ for aluminium and 234.5℃ for copper).

Under steady state condition, the heat-balance equation expressed the relationship between conductor temperature and current [10].

$$Q_J = Q_C + Q_R - Q_S \quad (2)$$
$$Q_J = I^2 R(T_C) \quad (3)$$
$$I^2 R(T_C) = Q_C + Q_R - Q_S \quad (4)$$

Where
$R(T_C)$ is the conductor resistance at temperature T_C,
I is the load current,
Q_J is the resistive heat gain due to loss,
Q_C is the convection heat loss,
Q_R is the radiated heat loss,
Q_S is the solar heat gain.

2.1 Convective heat loss

Convective heat loss is the effect of heat transfer due to air passing in contact with a metal conductor. Based upon wind velocity it is classified as natural convection and forced convection. The magnitude of Q_C is the function of dimensionless number known as Reynolds number [11].

$$N_{Re} = (D_0 . \delta_f . V_w)/\mu_f \quad (5)$$

$$Q_C = K_{Angle} \{1.01 + 1.35 N_{Re}^{0.52}\} K_f (T_c - T_a) \quad (6)$$

Where

N_{Re} : Reynolds number

D_0 : Conductor diameter

δ_f : Air density

V_w : wind velocity

μ_f : Dynamic viscosity of air

T_a : Ambient air temperature

T_c: Conductor surface temperature

K_{Angle} : Wind direction factor

K_f : Thermal conductivity of air at temperature Tfilm

2.2 Radiated heat loss

Radiated heat loss is the energy transmitted through radiation to the surrounding when the conductor heated up above the ambient temperature. Its magnitude depends upon conductor geometry, temperature difference of conductor and surrounding.

$$Q_R = 17.8 * D_0 * \varepsilon \left[\left(\frac{T_c+273}{100} \right)^4 - \left(\frac{T_a+273}{100} \right)^4 \right] \quad (7)$$

2.3 Solar heat gain

Solar heat gain is the energy provided by the sun to the conductor and it depends upon sun's position, solar constant, orientation of the conductor and its absorptivity.

$$Q_s = \alpha . Q_{se} . \sin\theta . A' \quad (8)$$

2.4 Resistive heat gain

Resistive heat gain is the function of real loss of the conductor. Its magnitude depends upon current flowing through the conductor and its ac resistance at that temperature.

$$Q_J = I^2 R \quad (9)$$

$$Q_J = I^2 \, R_{ref} \frac{T_C + T_F}{T_{ref} + T_F} \quad (10)$$

Solar heat gain is depend upon solar radiation but other three terms i.e Q_J, Q_C and Q_R all are the nonlinear function of line temperature. But under normal weather and operating condition Q_C and Q_R may be represented as :

$$Q_C \approx K_C (T_C - T_{Amb}) \quad (11)$$

$$Q_R \approx K_R (T_C - T_{Amb}) \quad (12)$$

And using $Q_J = P_{Loss}$ (13)

Conductor temperature estimated as[12]:

$$T_C = T_{Amb} + \frac{P_{Loss} + Q_s}{K_C + K_R} \quad (14)$$

After solving equation (14) conductor temperature for a given conductor current and weather condition will be computed. And putting this value in equation (1) conductor resistance has to be computed at temperature T_C.

3 Load Flow Analysis

Load flow algorithm developed by ranjan et el [13] is modified by incorporating uncertainty in the line resistance. As described above the resistance is the function of temperature and its value vary according to the temperature and weather condition.

3.1 Mathematical model of radial distribution system

Mathematical model of RDS can be derived from Fig.1[13]

$$I(jj) = \frac{|V(m1)| \angle\delta(m1) - |V(m2)| \angle\delta(m2)}{Z(jj)} \quad (15)$$

$$P(m2) - jQ(m2) = V^*(m2) * I(jj) \quad (16)$$

$$|V(m2)| = \sqrt{\{B(jj) - A(jj)\}} \quad (17)$$

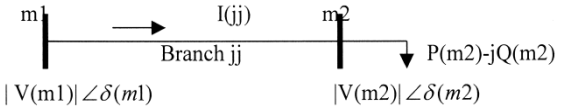

Fig.1

$$A(jj) = P(m2)*R(jj) + Q(m2)*X(jj) - 0.5*|V(m1)|^2 \quad (18)$$

$$B(jj) = \sqrt{\left[A^2(jj) - \{Z^2(jj) * (P^2(m2) + Q^2(m2))\}\right]}. \quad (19)$$

$$P_L(jj) = \frac{R(jj) * (P^2(m2) + Q^2(m2))}{|V(m2)|^2} \quad (20)$$

$$Q_L(jj) = \frac{X(jj) * (P^2(m2) + Q^2(m2))}{|V(m2)|^2} \quad (21)$$

Where

Z(jj)= R(jj)+jX(jj) impedance of the branch (jj), m1 and m2 are the sending and receiving end node, V(m1) and V(m2) are the sending and receiving end node voltage, P(m2) is the sum of real power loads of the nodes beyond the node m2 plus the sum of the real power losses of the nodes beyond the node m2 plus the real power load of the node m2 itself and Q(m2) is the sum of reactive power loads of the nodes beyond the node m2 plus the sum of the reactive power losses of the nodes beyond the node m2 plus the reactive power load of the node m2 itself. $P_L(jj)$ and $Q_L(jj)$ are real and reactive power loss of the branch (jj).

After solving the above equations, systems real and reactive losses, node voltage and branch current have to be calculated.

3.2 Modified load flow algorithms

Computing the load flow solution, and hence line losses, requires obviously that conductor resistance shall be specified. However, as discussed above, such resistance is the nonlinear function of the current and temperature. Therefore conventional load flow analysis tools required to be modified, unless conductor temperature is specified in the input data.

i) Line resistance in the input data are set to an initial value i.e corresponding with $T_C = 20^0C$.

ii) Solve the conventional load flow equations (15) -(21) and find out the current, node voltage and system losses.
iii) Based on those results and local weather condition given in table 4, conductor temperature is estimated by solving equation (14).
iv) Line resistances are updated by solving equation (1). If no significant changes in line resistance are observed for two successive iterations then stop. Otherwise go to step (ii).
v) At last find the results of load flow equations and the conductor temperature for each branch.

4 Results and Discussion

To check the efficiency and effectiveness of the proposed algorithm with temperature dependence it has been tested on several RDS and for the constraint of space in paper IEEE 69 bus system results are analyzed. The type of conductor used for the test system is given in table 1. The test system is shown in Fig.6 and the input line and load data in table 6 [13].
For load flow calculation, the base power is 100MVA and the base voltage is 12.66KV. For conventional load flow the convergence criterion of voltage is 0.0001V. The convergence criterion of resistance is 0.00001 ohm. Temperature constant T_F is material dependent and all the conductor of test system are assumed as made up of hard drawn aluminum with temperature constant 228.1℃. For the calculation of the solar heat gain, convective heat loss and radiated heat loss the input data is taken from the table 3.

Table 1: Conductor selection [14]

Conductor type	Branch number
Hyena	From 1 to 26
Dog	Rest of 68 branches

Comparative results of Conventional load flow algorithm and Weather Sensitive Load Flow (WSLF) algorithm for test system (IEEE 69 Bus system) are given in table 2. The real power losses are increased by nearly 15% and minimum voltage at node 65 is decreased by 1% approx. as compared to the conventional load flow. This is because the change in the branch resistance of the conductor as shown in Fig 2. The branch resistance of the conductor is increased by 12% as compared to the initial resistance.

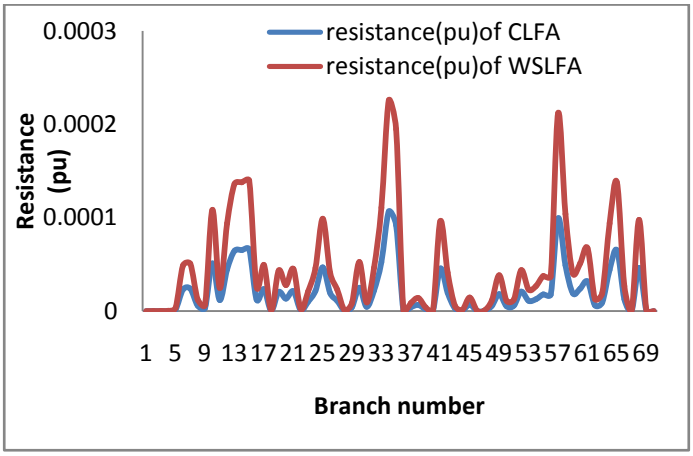

Fig.2 comparative results of branch resistances

Table 2: Comparative results of Conventional load low algorithm and Weather Sensitive Load Flow (WSLF) algorithm for test system (IEEE 69 Bus system)

Conventional load flow		WSLF		%Change	
Real power loss (kW)	Vmin (pu)	Real power loss(Kw)	Vmin (pu)	Real power loss	Voltage
230.77	V_{65}= 0.9079	264.68	V_{65}= 0.8978	14.69	1.11

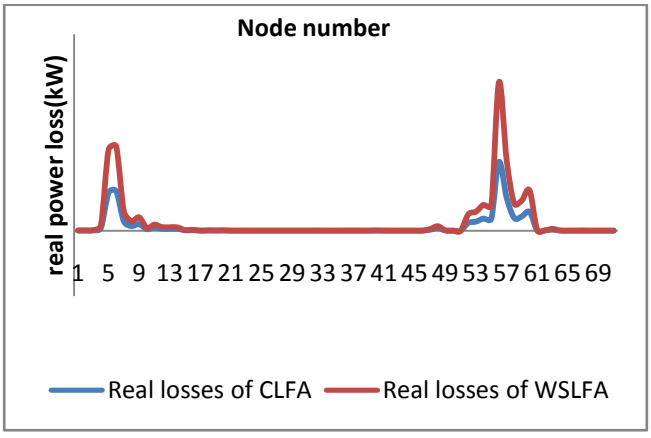

Fig.3 the comparative results of real power losses of each branch

Fig 3 presents the comparative result of real power losses of each branch of test system (IEEE 69 Bus system). With increase in branch temperature, the change of losses basically increase till the branch temperature become constant for a particular weather condition and load current [15]. This is because the branch temperature is the function of local weather condition and current flowing through it.

Fig.4 presents the comparative results of node voltages of the test system. V1 and V2 are the per unit node voltages calculated by conventional load flow method and proposed load flow algorithm respectively. As the branch resistance increase, the voltage drops. So the node voltages decrease with rise in the branch temperature and became constant when the rise in temperature is negligible.

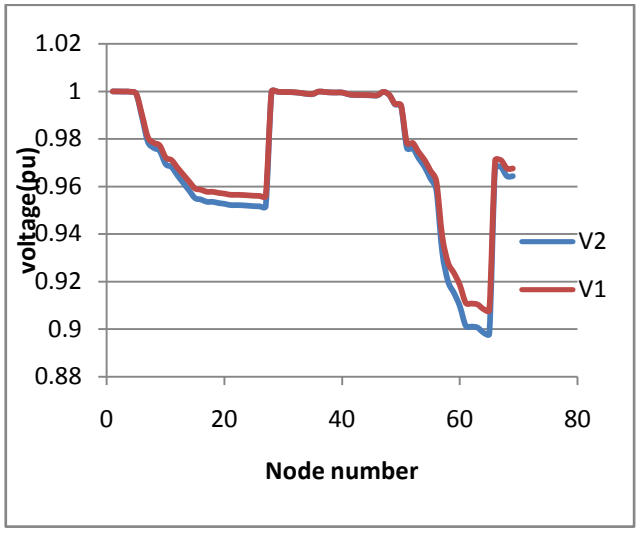

Fig. 4 the comparative results of node voltages of the test system.

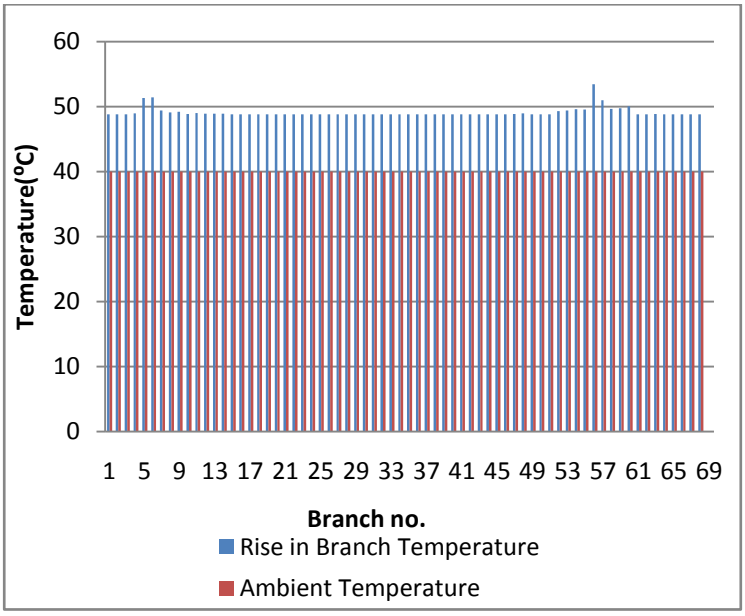

Fig 5. The comparative results of ambient temperature and rise in branch temperature of the test system

The detailed results obtained from the proposed weather sensitive load flow algorithm are given in table 3. The real power losses mentioned in [13] is 224.9606 kW and the loss calculated by the proposed algorithm is 264.68Kw. Table 3 compare the relative change for conductor resistance, real power losses and node voltages.

Table 3: Detailed Branch Wise Results for IEEE 69 Bus system

Br. No	Send. node	Rec. node	Resistance (per unit)			Active losses (kW)			Node voltage (per unit)		
			conventional load flow	weather sensitive load flow	% Change	conventional load flow	weather sensitive load flow	% Change	conventional load flow	weather sensitive load flow	% Change
1	1	2	0.00000003	0.00000003	11.61	0.0752	0.0847	12.70	0.999967	0.9999648	0.0002
2	2	3	0.00000003	0.00000003	11.61	0.0752	0.0847	12.70	0.999933	0.9999296	0.0003
3	3	4	0.00000009	0.00000010	11.62	0.1955	0.2205	12.78	0.999839	0.9998316	0.0007
4	4	5	0.00000157	0.00000175	11.68	1.9467	2.2036	13.20	0.999018	0.9989522	0.0066

5	5	6	0.00002284	0.00002572	12.62	28.8593	32.9975	14.34	0.989984	0.9889899	0.1004
6	6	7	0.00002378	0.00002679	12.66	30.0146	34.3441	14.42	0.980584	0.9786207	0.2002
7	7	8	0.00000575	0.00000643	11.85	6.9484	7.8857	13.49	0.978359	0.9761818	0.2226
8	8	9	0.00000308	0.00000344	11.73	3.3943	3.8490	13.40	0.977223	0.9749363	0.2340
9	9	10	0.00005110	0.00005712	11.78	4.8312	5.4453	12.71	0.972193	0.969398	0.2875
10	10	11	0.00001168	0.00001304	11.65	1.0179	1.1452	12.50	0.971089	0.9681851	0.2991
11	11	12	0.00004439	0.00004957	11.69	2.2086	2.4880	12.65	0.967916	0.9646923	0.3330
12	12	13	0.00006426	0.00007175	11.65	1.2962	1.4609	12.71	0.964979	0.9614588	0.3648
13	13	14	0.00006514	0.00007273	11.65	1.2554	1.4150	12.72	0.96207	0.9582548	0.3965
14	14	15	0.00006601	0.00007370	11.65	1.2141	1.3686	12.72	0.959189	0.9550832	0.4281
15	15	16	0.00001227	0.00001369	11.62	0.2245	0.2529	12.64	0.958656	0.9544958	0.4339
16	16	17	0.00002336	0.00002607	11.62	0.3217	0.3624	12.66	0.957774	0.9535254	0.4436
17	17	18	0.00000029	0.00000033	11.61	0.0026	0.0029	12.63	0.957765	0.9535156	0.4437
18	18	19	0.00002044	0.00002281	11.61	0.1045	0.1178	12.65	0.9573	0.9530039	0.4487
19	19	20	0.00001314	0.00001467	11.61	0.0672	0.0757	12.65	0.957	0.9526751	0.4520
20	20	21	0.00002131	0.00002379	11.61	0.1078	0.1215	12.65	0.956518	0.9521446	0.4572
21	21	22	0.00000087	0.00000097	11.61	0.0005	0.0006	12.65	0.956511	0.952137	0.4573
22	22	23	0.00000993	0.00001108	11.61	0.0051	0.0058	12.65	0.956439	0.952058	0.4581
23	23	24	0.00002161	0.00002412	11.61	0.0112	0.0126	12.65	0.956283	0.9518861	0.4597
24	24	25	0.00004672	0.00005214	11.61	0.0061	0.0068	12.65	0.956113	0.9517002	0.4616
25	25	26	0.00001927	0.00002151	11.61	0.0025	0.0028	12.65	0.956044	0.9516235	0.4623
26	26	27	0.00001081	0.00001206	11.61	0.0003	0.0004	12.65	0.956024	0.951602	0.4625
27	3	28	0.00000027	0.00000031	11.61	0.0003	0.0004	11.58	0.999926	0.9999224	0.0004
28	28	29	0.00000399	0.00000446	11.61	0.0026	0.0029	11.58	0.999854	0.9998477	0.0007
29	29	30	0.00002482	0.00002770	11.61	0.0058	0.0065	11.59	0.999733	0.9997151	0.0018
30	30	31	0.00000438	0.00000489	11.61	0.0010	0.0011	11.59	0.999712	0.9996918	0.0020
31	31	32	0.00002190	0.00002444	11.61	0.0051	0.0057	11.59	0.999605	0.9995748	0.0030
32	32	33	0.00005235	0.00005843	11.61	0.0123	0.0137	11.60	0.999349	0.9992946	0.0054
33	33	34	0.00010657	0.00011894	11.61	0.0104	0.0116	11.60	0.999013	0.9989274	0.0086
34	34	35	0.00009197	0.00010264	11.61	0.0005	0.0005	11.62	0.998946	0.9988536	0.0092
35	3	36	0.00000027	0.00000031	11.61	0.0014	0.0016	11.58	0.999919	0.9999152	0.0004
36	36	37	0.00000399	0.00000446	11.61	0.0151	0.0168	11.59	0.999747	0.999736	0.0011
37	37	38	0.00000657	0.00000733	11.61	0.0173	0.0193	11.59	0.999589	0.9995672	0.0022
38	38	39	0.00000190	0.00000212	11.61	0.0050	0.0056	11.59	0.999543	0.9995185	0.0025
39	39	40	0.00000011	0.00000013	11.61	0.0002	0.0002	11.59	0.999541	0.9995162	0.0025
40	40	41	0.00004544	0.00005072	11.61	0.0488	0.0544	11.61	0.998843	0.9987727	0.0070
41	41	42	0.00001934	0.00002159	11.61	0.0201	0.0225	11.60	0.99855	0.9984613	0.0089
42	42	43	0.00000256	0.00000286	11.61	0.0027	0.0030	11.59	0.998511	0.9984201	0.0091
43	43	44	0.00000057	0.00000064	11.61	0.0005	0.0006	11.59	0.998503	0.9984113	0.0092
44	44	45	0.00000679	0.00000758	11.61	0.0061	0.0068	11.60	0.998405	0.9983066	0.0098
45	45	46	0.00000006	0.00000006	11.61	0.0000	0.0000	11.59	0.998404	0.9983061	0.0098
46	4	47	0.00000021	0.00000024	11.61	0.0233	0.0260	11.62	0.999789	0.9997794	0.0010
47	47	48	0.00000531	0.00000593	11.63	0.5843	0.6524	11.65	0.998541	0.9984787	0.0062

48	48	49	0.00001808	0.00002019	11.67	1.6463	1.8393	11.72	0.994675	0.9944487	0.0228
49	49	50	0.00000513	0.00000572	11.61	0.1160	0.1295	11.64	0.99413	0.9938802	0.0251
50	8	51	0.00000579	0.00000646	11.61	0.0018	0.0020	12.07	0.978324	0.9761432	0.2229
51	51	52	0.00002071	0.00002311	11.61	0.0000	0.0000	12.07	0.978314	0.9761328	0.2230
52	9	53	0.00001086	0.00001214	11.81	5.8397	6.6491	13.86	0.974422	0.9718605	0.2628
53	53	54	0.00001267	0.00001417	11.85	6.7858	7.7305	13.92	0.97116	0.9682781	0.2968
54	54	55	0.00001773	0.00001985	11.93	9.2501	10.5522	14.08	0.966656	0.9633254	0.3445
55	55	56	0.00001755	0.00001964	11.92	8.9095	10.1659	14.10	0.962257	0.9584889	0.3916
56	56	57	0.00009920	0.00011257	13.47	52.3884	60.9406	16.32	0.93913	0.9324732	0.7088
57	57	58	0.00004890	0.00005501	12.50	25.1670	28.9584	15.07	0.927906	0.9199643	0.8559
58	58	59	0.00001898	0.00002125	11.95	9.6233	11.0049	14.36	0.9236	0.915189	0.9107
59	59	60	0.00002409	0.00002698	11.99	10.8212	12.3869	14.47	0.918537	0.9095636	0.9769
60	60	61	0.00003166	0.00003550	12.11	14.2990	16.3983	14.68	0.911067	0.9013362	1.0681
61	61	62	0.00000608	0.00000678	11.61	0.1124	0.1282	14.06	0.910777	0.901018	1.0715
62	62	63	0.00000905	0.00001010	11.61	0.1354	0.1545	14.07	0.910389	0.9005919	1.0761
63	63	64	0.00004433	0.00004949	11.63	0.6658	0.7599	14.13	0.908482	0.8984992	1.0988
64	64	65	0.00006495	0.00007249	11.61	0.0414	0.0472	14.09	0.907906	0.8978678	1.1057
65	11	66	0.00001255	0.00001401	11.61	0.0026	0.0029	12.24	0.971033	0.9681228	0.2997
66	66	67	0.00000029	0.00000033	11.61	0.0000	0.0000	12.24	0.971032	0.9681221	0.2997
67	12	68	0.00004613	0.00005149	11.61	0.0234	0.0262	12.34	0.967585	0.96433	0.3364
68	68	69	0.00000029	0.00000033	11.61	0.0000	0.0000	12.33	0.967584	0.9643288	0.3365

5 Conclusion

Overhead conductor temperature is the function of power transmitted and weather condition. Conventional load flow ignored this effect and take the value of resistances at specified certain temperatures. To improve the efficiency of the load flow calculation, weather sensitive load flow algorithm is proposed. The effectiveness of the algorithm is tested on several RDS and for the purpose of demonstration results of IEEE 69 Bus system is included in the paper.

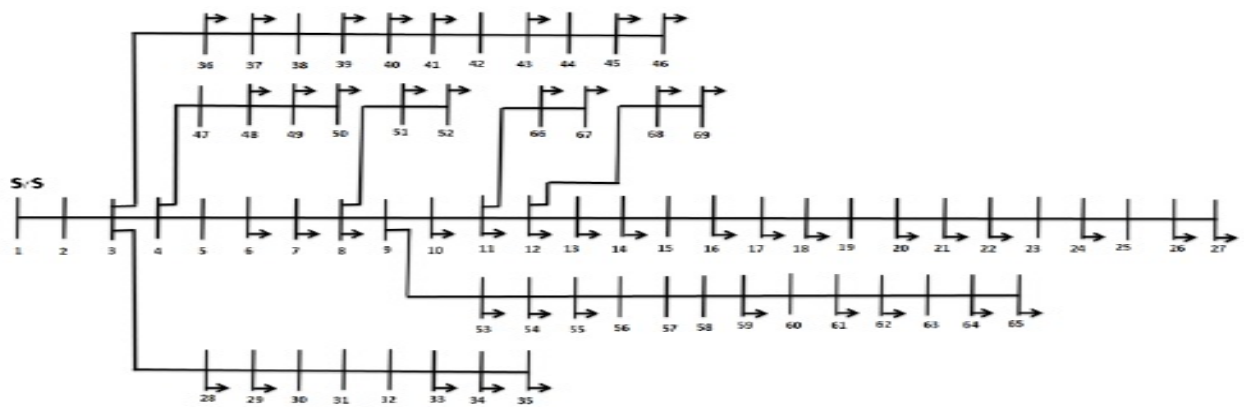

Fig. 6 IEEE 69 bus test system

References:

[1] J.Nanda , M.S.Srinivas, M.Shma, S.S.Dev and L.L.Lai, "New Findings on Radial Distribution System Load Flow Algorithms" IEEE conference, 2000 pp.1157-1161

[2] B. Venkatesh and R. Ranjan, " Data structure for radial distribution system load flow analysis", IEE Prociding -Gener. Trans. Distrib. Vol.150. No 1. January 2003.

[3] T. Thakur and Jaswanti Dhiman, "A New Approach to Load Flow Solutions for Radial Distribution System", IEEE conference, 2006.

[4] G. W. Chang, S. Y. Chu and H. L. Wang, "An Improved Backward/Forward Sweep Load Flow Algorithm for Radial Distribution Systems" IEEE TRANSACTIONS ON POWER SYSTEMS, VOL. 22, NO. 2, MAY 2007, pp 882-884.

[5] Robert A. Maraio and Stephen D. FOSS, "effect of variability in weather conditions on conductor temperature and the dynamic rating of transmission lines", IEEE Transactions on Power Delivery, Vol. 3, No. 4, October 1988,pp.1832-1841.

[6] Hadi Banakar, Natalia Alguacil and Francisco D. aliana,"Electrothermal Coordination Part I: Theory and Implementation Schemes," IEEE Transactions on Power Systems, Vol. 20, NO. 2, MAY 2005, pp. 798-805.

[7] Natalia Alguacil, M. Hadi Banakar,and Francisco D. Galiana, "Electrothermal Coordination Part II: Case Studies," IEEE Transactions on Power Systems, Vol. 20, NO. 4, November 2005,pp.1738-1745.

[8] Marija Bockarjova and Goran Andersson, "Transmission Line Conductor Temperature Impact on State Estimation Accuracy," Power Tech, 2007 IEEE Lausanne, Switzerland.

[9] S.Frank, J. Sexauer, and S. Mohagheghi, "Temperature Dependent Power Flow," IEEE Trans. Power Syst., vol. 28, pp. 4007-4018, Oct. 2013

[10] J.R. Santos, A. G!omez Exposito and F. Parreno Sanchez, "Assessment of conductor thermal models for grid studies," IET Gener. Transm. Distrib., Vol. 1, No. 1, January 2007, pp.155-161.

[11] IEEE Standard for Calculating the Current-Temperature of Bare Overhead Conductors, IEEE Std. 738, 2006.

[12] Qin Gao, Zhinong Wei, Guoqiang Sun, Yonghui Sun, and Haixiang Zang, "Temperature- Depended Optimal Power Flow Based on Simolified Interior Point Method," 5th international conference on Electric Utility Deregulation and Restructuring and Power Technologies, nov. 26-29, 2015, pp 765-769.

[13] R. Ranjan and D. Das, "Simple and Efficient Computer Algorithm to Solve Radial Distribution Networks," Electric Power Components and Systems, 31:95–107, 2003.

[14] Mahdi Mozaffari Legha , Hassan Javaheri and Mohammad Mozaffari Legha,"Optimal Conductor Selection in Radial Distribution Systems for Productivity Improvement Using Genetic Algorithm", Iraq J. Electrical and Electronic Engineering, Vol.9 No.1 , 2013.

[15] H.T. Jadhav and P.D. Bamane , "Temperature dependent optimal power flow using g-best guided artificial bee colony algorithm," Electrical Power and Energy Systems 77 (2016) 77–90, pp.77-90.

APPENDIX: A

Table 4

Input Parameters	**ACSR (Hyena)**	**ACSR (Dog)**
Wind speed (V_w)	0.61 m/s	0.61 m/s
Conductor elevation (m)	0	0
Emissivity (ε)	0.8	0.8
Solar absorptivity (α)	0.8	0.8
Ambient temperature (T_a)	40 °C	40 °C

Maximum temperature (T_c)	100°C	100°C
Latitude (°)	30°N	30°N
Conductor outer diameter (D0)	14.57 mm	14.15 mm
Conductor inner diameter (d_0)	4.39 mm	4.72 mm
Angle between conductor axis and wind direction (°)	90	90
Day number	161	161
Solar declination (δ)	23°	23°
Hour angle (w) at 11:00am	-15°	-15°
Solar heat intensity Q_{se}	1027 W/m^2	1027 W/m^2
Solar azimuth angle (Z_c)	114°	114°
Angle of incidence of the sun rays with conductor axis (ɵ)	76.1°	76.1°
DC resistance at 20°C (Ω/km)	0.1576	0.2712
Dynamic viscosity of air (μ_f)	2.043 x10^{-5} kg/m-s	2.043 x10^{-5} kg/m-s
Thermal conductivity of air at temperature Tfilm (K_f)	0.02945 W/m-°C	0.02945 W/m-°C
Wind direction factor (K_{Angle})	1	1
Air density (δ_f)	1.029 kg/m^3	1.029 kg/m^3

Table 5

ACSR Code Word	Cond. Area mm2	Stranding& Wire Dia in mm		Calculated sectional Area Sq.mm		Approx overall Dia mm	Weight kg/km			Calc. Electrical Resistance at 20oC Ohms/km	Approx Calc. Breaking Load(KN)
		Alum.	Steel	Alum.	ACSR	ACSR	ACSR	Alum.	Steel	Cond.	Cond.
MOLE	10	6/1.50	1/1.50	10.6	12.37	4.5	43	29	14	2.78	3.97
SPECIAL	18	6/1.95	1/1.95	18.1	21.12	5.88	73	50	23	1.618	6.74
SQUIRREL	20	6/2.11	1/2.11	20.98	24.48	6.33	85	58	27	1.394	70.61
WEASEL	30	6/2.59	1/2.59	31.61	36.88	7.77	128	87	41	0.929	11.12
RABBIT	50	6/3.35	1/3.35	52.88	61.7	10.05	214	145	69	0.552	18.25
RACCOON	80	6/4.09	1/4.09	78.83	91.97	12.27	319	216	103	0.371	26.91
DOG	100	6/4.72	7/1.57	105	118.5	14.15	394	288	106	0.279	32.41
WOLF	150	30/2.59	7/2.59	158.1	194.9	18.13	726	437	289	0.187	67.34

PANTHER	200	30/3.0	7/3.00	212.1	261.5	21	974	586	388	0.139	89.67
KUNDAH	400	42/3.50	7/1.96	404.1	425.2	26.88	1281	1116	165	0.073	88.79
ZEBRA	420	54/3.18	7/3.18	428.9	484.5	28.62	1621	1186	435	0.069	130.32
MOOSE	520	54/3.53	7/3.53	528.5	597	31.77	2004	1461	537	0.056	161.2
MORKULLA	560	42/4.13	7/2.30	562.7	591.7	31.68	1787	1553	228	0.052	120.16

Table 6.

Branch no	Send. node	Rec. node	R(ohm)	X(ohm)	Real Load(kW)	Reactive Load(kVAr)
1	1	2	0.0005	0.0012	0	0
2	2	3	0.0005	0.0012	0	0
3	3	4	0.0015	0.0036	0	0
4	4	5	0.0251	0.0294	0	0
5	5	6	0.366	0.1864	2.6	2.2
6	6	7	0.3811	0.1941	40.4	30
7	7	8	0.0922	0.047	75	54
8	8	9	0.0493	0.0251	30	22
9	9	10	0.819	0.2707	28	19
10	10	11	0.1872	0.0619	145	104
11	11	12	0.7114	0.2351	145	104
12	12	13	1.03	0.34	8	5.5
13	13	14	1.044	0.345	8	5.5
14	14	15	1.058	0.3496	0	0
15	15	16	0.1966	0.065	45.5	30
16	16	17	0.3744	0.1238	60	35
17	17	18	0.0047	0.0016	60	35
18	18	19	0.3276	0.1083	0	0
19	19	20	0.2106	0.0696	1	0.6
20	20	21	0.3416	0.1129	114	81
21	21	22	0.014	0.0046	5.3	3.5
22	22	23	0.1591	0.0526	0	0
23	23	24	0.3463	0.1145	28	20
24	24	25	0.7488	0.2475	0	0
25	25	26	0.3089	0.1021	14	10
26	26	27	0.1732	0.0572	14	10
27	3	28	0.0044	0.0108	26	18.6
28	28	29	0.064	0.1565	26	18.6
29	29	30	0.3978	0.1315	0	0
30	30	31	0.0702	0.0232	0	0
31	31	32	0.351	0.116	0	0
32	32	33	0.839	0.2816	14	10
33	33	34	1.708	0.5646	19.5	14
34	34	35	1.474	0.4873	6	4
35	3	36	0.0044	0.0108	26	18.55
36	36	37	0.064	0.1565	26	18.55
37	37	38	0.1053	0.123	0	0
38	38	39	0.0304	0.0355	24	17
39	39	40	0.0018	0.0021	24	17

40	40	41	0.7283	0.8509	1.2	1
41	41	42	0.31	0.3623	0	0
42	42	43	0.041	0.0478	6	4.3
43	43	44	0.0092	0.0116	0	0
44	44	45	0.1089	0.1373	39.22	26.3
45	45	46	0.0009	0.0012	39.22	26.3
46	4	47	0.0034	0.0084	0	0
47	47	48	0.0851	0.2083	79	56.4
48	48	49	0.2898	0.7091	384.7	274.5
49	49	50	0.0822	0.2011	384.7	274.5
50	8	51	0.0928	0.0473	40.5	28.3
51	51	52	0.3319	0.1114	3.6	2.7
52	9	53	0.174	0.0886	4.35	3.5
53	53	54	0.203	0.1034	26.4	19
54	54	55	0.2842	0.1447	24	17.2
55	55	56	0.2813	0.1433	0	0
56	56	57	1.59	0.5337	0	0
57	57	58	0.7837	0.263	0	0
58	58	59	0.3042	0.1006	100	72
59	59	60	0.3861	0.1172	0	0
60	60	61	0.5075	0.2585	1244	888
61	61	62	0.0974	0.0496	32	23
62	62	63	0.145	0.0738	0	0
63	63	64	0.7105	0.3619	227	162
64	64	65	1.041	0.5302	59	42
65	11	66	0.2012	0.0611	18	13
66	66	67	0.0047	0.0014	18	13
67	12	68	0.7394	0.2444	28	20
68	68	69	0.0047	0.0016	28	20